Mechanistic aspects of the release and the reduction of NO_x stored on $Pt–Ba/Al_2O_3$

L. Castoldi, L. Righini, R. Matarrese, L. Lietti *, P. Forzatti *

Dipartimento di Energia, Laboratory of Catalysis and Catalytic Processes and NEMAS, Centre of Excellence, Politecnico di Milano, P.zza L. da Vinci 32, Milano, Italy

Received 29 September 2014
Revised 27 December 2014
Accepted 9 February 2015
Available online 7 March 2015

This paper is dedicated to Dr. Haldor Topsøe as a recognition to his pioneeristic activities in the field of environmental catalysis.

1. Introduction

The need in industrialized countries to improve the fuel economy and to reduce CO_2 emissions in the transportation sector has motivated the spreading of diesel vehicles and lean burn DI (Direct Injection) gasoline vehicles, due to the intrinsic more effec-tive combustion realized under lean conditions. While compliance with previous NO_x regulatory limits has been achieved for these vehicles mostly without resort to NO_x after treatments, technolo-gies like the selective catalytic reduction (SCR) or the NO_x storage reduction (NSR) are required to achieve the most severe present and upcoming NO_x emission standards in USA, EU, and Japan [1,2]. The NH_3/urea SCR is recognized as the most effective tech-nology for the abatement of NO_x emissions from HD (Heavy Duty) diesel vehicles, and a growing interest in the same tech-nology is coming also from LD (Light Duty) vehicles and passenger cars. The NSR, also referred as Lean NO_x Traps (LNT), is a favoured approach for lighter vehicles, mainly because of the fact that no big layout modifications are needed and of the relatively fixed cost of the on-board urea system [2,3].

The NSR system is operated in a cyclic manner by alternating long lean phases (e.g., 60–90 s) to trap NO_x with short rich phases (e.g., 3–5 s) to regenerate the catalyst. A typical NSR catalyst comprises an alkaline earth and/or alkaline component such as barium and/or potassium to trap the NO_x, a PGM (Platinum Group Metal) such as Pt with Rh (and Pd) to oxidize NO, CO and unburned hydrocarbons and to reduce trapped NO_x producing nitrogen, and a high surface area support, such as alumina, where the catalyst components are dispersed.

The overall principle of operation of NSR has been described by the following steps [4]: (i) oxidation of NO to NO_2; (ii) NO and/or NO_2 up-take in the form of nitrites and/or nitrates; (iii) injection/formation of the reducing agents when the exhaust is switched to rich conditions; (iv) reduction of the stored nitrites and nitrates to N_2 and other by-products.

The reduction of the stored NO_x is a rather complex process that has not yet been fully understood. It is generally believed that the reduction initially involves the so-called release of the stored NO_x in the form of gaseous NO_x and/or as adsorbed species on Pt, which are then reduced over Pt to N_2 and other by-products [4]. Different driving forces have been invoked to explain the NO_x release. Some authors [5,6] proposed that the NO_x are released as a result of the heat generated by the combustion of the reductants upon the lean/rich switch. Indeed, as the rich front passes over the catalyst and the surface temperature increases, stored NO_x can be released because their stability decreases with increasing temperature. Other authors [7,8] have proposed that the release of NO_x is caused by a decrease in the stability of the stored NO_x driven by

* Corresponding authors.
E-mail addresses: luca.lietti@polimi.it (L. Lietti), pio.forzatti@polimi.it (P. Forzatti).

adsorption–desorption equilibrium due to the decrease in the partial pressure of oxygen and/or of NO upon the lean/rich switch. Finally, it has been suggested that the establishment of a net reducing environment causes the formation of reduced Pt sites that reduce the stored nitrites and nitrates to form primarily NO [4,9,10]. According to Shakya et al. [11], the NO_x release process occurs at the Pt/Ba interface and therefore involves NO_x species stored close to Pt sites. Accordingly, NO_x species adsorbed far away from Pt must first spill to the reduced noble metal sites before being released, as suggested by Clayton et al. [12] for catalysts having poor Pt dispersion. The spillover of H_2 activated over Pt sites towards the Ba sites has also been invoked as a possible pathway leading to the release of the stored NO_x species as gaseous NO [11].

Whatever mechanism is involved in the release of stored NO_x, during typical NSR operation it is not possible to decouple the release of NO_x from its further reduction to N_2 and other by-products, because the reduction of released NO_x is a very fast reaction. This prevents the unambiguous characterization of the NO_x release process. Most commonly, these two steps are considered as sequential steps, and the process of NO_x release is associated to the breakthrough of desorbed but unconverted NO_x upon the lean-rich switch (NO puff). Accordingly, the detection of unconverted NO_x during the rich phase implies that the rate of reduction is slower than the rate of release. This has been attributed either to the slow reduction of the precious metal sites responsible for the reduction of NO_x to N_2 and other by-products in comparison with the decomposition of the Ba nitrates/nitrites, to the release of NO_x from Ba sites far away from Pt (these species must spillover towards Pt sites before they are released) and to the large amount of NO_x released in a very short time period [4].

In this work, we intended to investigate in details the chemistry behind the NO_x release process over a model LNT Pt–Ba/Al_2O_3 catalyst having a high Pt dispersion, where spillover phenomena are expected to be of minor importance. For this purpose, different experiments have been carried out to investigate the relevance of the various routes suggested in the literature for the NO_x release. Since both nitrites and nitrates can be stored on the catalyst surface during the lean phase, as pointed out by several spectroscopic studies [see e.g., [13,14]], the behavior of these two species has been investigated. Accordingly, the thermal stability of stored nitrites and nitrates has been analyzed by means of the temperature-programmed desorption (TPD) method, while the impact of gas-phase NO and O_2 on the adsorption–desorption equilibrium of stored NO_x during the lean-rich switch has been studied by imposing a step change in the feed concentration of NO and O_2.

Isotopic exchange experiments between unlabeled stored $^{14}NO_x$ with labeled ^{15}NO (or vice versa) in the absence of oxygen have been used to probe the NO_x release process. In fact, having observed that the release of the stored NO_x results primarily in the evolution of NO in the gas phase, such exchange experiments have the potential for decoupling the release of the stored NO_x from the further reduction of the released NO. Indeed, during the exchange, the release of NO occurs in the absence of a reductant for NO, and hence, NO, once released, cannot be further reduced: this allows to unambiguously characterize the NO_x release process. In order to better clarify the role of Pt, NO isotopic exchange experiments have been carried out over a Pt-free Ba/Al_2O_3 catalyst as well. Notably, the exchange between ^{15}NO and stored $^{14}NO_x$ has already been used by Cant et al. [15] in the presence of O_2 to probe the forward and reverse spillover of NO_x species between Pt and BaO, and by Kumar et al. [16] to elucidate the role of spillover processes and to characterize the mobility of adsorbed NO_x as a function of the distance from Pt/BaO interphase.

Finally, the role of the reducing agent in the release and reduction of stored NO_x has been addressed by revisiting temperature-programmed surface reaction (TPSR) experiments of stored nitrates with different reductants, that is, with H_2, NH_3, CO and n-heptane. Notably, due to the low reductant concentration, the experiments have been carried out under nearly isothermal conditions, that is, in the absence of significant temperature gradients within the catalyst bed. This also obviously applies for TPD and isotopic exchange experiments. Accordingly, the intrusion of thermal effects in the study of the release process can be safely neglected.

As will be discussed below, it is found that the NO_x release is a chemical process, driven by reduced Pt sites and occurring at Pt/Ba interface.

2. Experimental

2.1. Catalysts preparation and characterization

A Pt–Ba/Al_2O_3 (1/20/100 w/w) catalyst has been prepared by incipient wetness impregnation of a commercial alumina sample (Versal 250 from UOP) with an aqueous solution of dinitro-diammine platinum (Strem Chemicals, 5% Pt in ammonium hydroxide) and then with a solution of barium acetate (Aldrich, 99%). The powder has been dried at 80 °C overnight and calcined in air at 500 °C for 5 h after each impregnation step. The impregnation order (first Pt and then Ba) has been chosen in order to ensure a good dispersion and stability of the noble metal and of the alkaline component on the alumina support, in line with the recipes of Toyota patents [17].

The specific surface area of the sample measured by the BET method (Micromeritics TriStar 3000 instrument) is near 160 $m^2 g^{-1}$. The Pt dispersion was estimated by H_2 chemisorption at 0 °C (TPD/R/O 1100 Thermo Fischer instrument), and a value near 52% has been obtained. XRD diffraction spectra have been recorded with a Philips PW 1050/70 diffractometer. The spectra show mainly the diffraction lines corresponding to microcrys-talline γ-Al_2O_3, barium carbonate orthorhombic, and monoclinic phases (in trace amounts), along with a small diffraction peak at $2\theta = 40°$ possibly related to the presence of Pt^0 [18].

A Pt-free Ba/Al_2O_3 (20/100 w/w) sample was also prepared for comparison purposes, using the same impregnation method.

2.2. Catalytic tests and methods

Catalytic tests have been carried out in a micro-reactor consisting of a quartz tube (7 mm I.D.), loaded with 60 mg of catalyst powder (70–100 μm). A total flow of 100 cm^3/min (at 1 atm and 0 °C) has been used in all the experiments, corresponding to a GHSV of 10^5 h^{-1}. The reactor was directly connected to a mass spectrometer (Thermostar 200, Pfeiffer), an UV-NO_x analyzer (LIMAS 11HW, ABB) and a micro-gas chromatograph (3000A, Agilent) in a parallel arrangement for analysis of the reaction prod-ucts. Feed gases are obtained from calibrated gas mixtures (e.g., 0.2% v/v ^{14}NO in He; 0.3% v/v ^{15}NO in He, ^{15}N isotopic abundance 98%) containing an inert tracer (Ar).

Temperature-programmed desorption (He-TPD), ^{15}NO temperature-programmed isotopic exchange (^{15}NO-TPIE), and temperature-programmed surface reaction (TPSR) experiments with different reductants (H_2, NH_3, CO, n-heptane) have been carried out in all cases after catalyst conditioning at 350 °C. This consists in performing few storage/regeneration cycles at 350 °C. NO_x are adsorbed by imposing a rectangular step feed of NO (1000 ppm) in flowing He + 3% v/v O_2 until catalyst saturation. Then, the NO and O_2 concentrations have been stepwise decreased to zero, fol-lowed by a He purge at the same temperature (350 °C). This leads to the desorption of weakly adsorbed NO_x species [19]. After the He purge, catalyst regeneration (rich phase) has been carried out with H_2 (2000 ppm in He). Conditioning lasted until a reproducible

behavior was obtained, and this typically required 3–4 adsorption/reduction cycles [20]. As previously shown, conditioning implies the almost complete transformation of the initially present $BaCO_3$ storage sites into $BaO/Ba(OH)_2$.

In a typical TPD experiment, the catalyst has been saturated at 150 °C or 350 °C upon step-wise admission to the reactor of NO (1000 ppm) + O_2 3% v/v in flowing He, up to steady state conditions. According to previous works [14,21], this results in the formation of nitrites and nitrates at 150 °C and 350 °C, respectively. Then, the catalyst has been purged with He at the same temperature of adsorption, cooled down to 50 °C under flowing He and eventually heated under temperature programming from 50 °C to 500 °C (10 °C/min). The catalyst was hold at this temperature for about 20 min; then, it was cooled down to 350 °C in He flow and eventually 2000 ppm H_2 were admitted to complete the removal of stored NO_x.

The evolution with temperature of the surface species arising upon adsorption at 150 °C has been also analyzed by *in situ* FT-IR spectroscopy. IR spectra have been obtained on a Nicolet Nexus Fourier Transform instrument equipped with a DTGS detector with a resolution of 4 cm^{-1} (number of scans 100). For FT-IR analysis, the pure catalyst powder has been compressed in a self-supporting disk (of about 13 mg) and placed in an IR cell connected to a conventional manipulation/outgassing ramp that allows the disk to stay, alternatively, in the IR beam path or inside an oven. NO_x storage was performed by admitting NO and O_2 (P_{NO} = 1 mbar; P_{O2} = 30 mbar) at 150 °C. After the storage phase, the catalyst was evacuated at 150 °C and then heated up to 500 °C, by taking spectra every 50 °C.

In the ^{15}NO temperature-programmed isotopic exchange (^{15}NO-TPIE) experiments, after the storage phase performed at 150 °C or 350 °C (with $^{14}NO/O_2$) as already described for TPD experiments, the catalyst has been cooled to 50 °C under He flow. Then, a rectangular step feed of labeled ^{15}NO (850 ppm) in flowing He has been imposed. After stabilization of the signals, the temperature has been linearly increased (heating rate 10 °C/min) up to 350 °C; when the steady state conditions have been reached, ^{15}NO was switched off. Eventually, H_2 (2000 ppm in He) was admitted to the catalyst at 350 °C in order to reduce the residual adsorbed NO_x species. In order to check the differences in the reactivity of labeled and unlabeled species, the exchange reaction between ^{14}NO and labeled stored $^{15}NO_x$ was also investigated, and differences have been found to be negligible.

In order to investigate the effect of Pt on the ^{15}NO isotopic exchange reaction, ^{15}NO-TPIE experiments have been carried out over the Pt-free Ba/Al_2O_3 catalyst and over the $Pt–Ba/Al_2O_3$ catalyst after poisoning of Pt sites with CO (2000 ppm in He) at 50 °C. In the former case, the storage has been accomplished upon adsorption of NO_x starting from NO_2 (1000 ppm in He) at 350 °C, by adjusting the exposure time of adsorption so that the amounts of the adsorbed NO_x (nitrates) are comparable to that obtained with NO/O_2 over the $Pt–Ba/Al_2O_3$ sample at the same temperature. In the second case, after NO_x adsorption at 150 °C and He purge at the same temperature, the catalyst has been cooled down to 50 °C and contacted with CO at the same temperature, thus leading to the adsorption of CO onto the Pt sites.

Temperature-programmed surface reaction (TPSR) experiments of unlabeled nitrates have been carried out with different reductants (H_2, NH_3, CO, n-heptane). After NO_x adsorption at 350 °C followed by He purge at the same temperature, the catalyst has been cooled to 50 °C under He flow. Then, the reductant has been admitted to the reactor at 50 °C, and the catalyst temperature has been linearly increased up to 400 °C (heating rate 10 °C/min, hold at 400 °C 1 h), while monitoring the concentration of the products exiting the reactor.

In all the experiments, the analysis of the reaction products has been carried out by simultaneous use of mass spectrometry, gas-chromatography (GC) and an UV–Vis analysis, along the procedure already described in detail elsewhere [22]. Calibrated gas cylinders were used to estimate calibration factors and cracking patterns of unlabeled species; calibration factors of labeled species have been obtained from cylinders (^{15}NO) or by dedicated experiments (e.g., lean-rich cycles with ^{15}NO leading to the formation of $^{15}NO_2$, $^{15}N_2$ and $^{15}NH_3$). In particular, the overall concentration of nitrogen oxides (^{14}NO + ^{15}NO) and of nitrogen dioxides ($^{14}NO_2$ + $^{15}NO_2$) estimated from mass spectrometer data were compared with that of UV–Vis analysis. N balances carried out on the various experiments and calculated at steady state close within an error ±5%.

3. Results and discussion

3.1. Effect of NO and O_2 partial pressure on the stability of stored NO_x

The decrease in the partial pressure of NO and/or oxygen upon the lean/rich switch can cause the release of NO_x from the catalyst surface, as already pointed out in previous works [19,20,23]. In fact, as shown in Fig. 1A, during the NO_x adsorption at 350 °C onto the $Pt–Ba/Al_2O_3$ catalyst, after NO shutoff at the end of the storage phase (t = 1840 s), both the NO and the NO_2 concentrations show a prolonged tail indicating that weakly adsorbed nitrates decompose and eventually desorb from the catalyst surface in the form of NO and NO_2. The process is very slow since after several minutes the concentrations of NO and of NO_2 at the exit of the reactor have not been decreased to zero. A smaller additional NO desorption peak is observed upon switching off the oxygen flow in the feed at $t \sim 3130$ s in Fig. 1A, that is, under He purge. The amount of stored nitrates before the NO shutoff is evaluated near 0.35 mmol/g_{cat}; the tail after NO and O_2 shutoff accounts for the desorption of roughly 32% of the stored NO_x.

The net release of NO_x upon NO and O_2 shutoff can be estimated by subtracting the NO inlet concentration to the NO_x reactor outlet concentration, thanks to the presence of the Ar inert tracer in the NO calibrated gas mixture (see Section 2). The results are shown in Fig. 1B: a very fast NO_x release is initially observed upon the NO shutoff, which, however, in a representative time period of the rich phase accounts for only a small fraction of the initially stored NO_x. In fact, during the first 5 s after the NO shutoff less than 1% of stored NO_x has been released. A similar behavior has been observed when nitrites are stored onto the catalyst at 150 °C (Fig. 1C and D). In fact, when NO first and O_2 later are switched off, a tail in NO_x concentration is observed and the amount of stored NO_x decreases from 0.323 mmol/g_{cat} down to 0.241 mmol/g_{cat} after the NO and O_2 shutoff. Again, in the first 5 s upon the NO shutoff less than 1% of the initially stored NO_x have been released (Fig. 1D).

Besides negligible amounts of initially stored NO_x have been released after O_2 shutoff for both nitrates (Fig. 1B) and nitrites (Fig. 1D).

It is concluded that the amounts of released NO_x driven by the adsorption–desorption equilibrium of stored NO_x and produced by the decrease in the partial pressure of NO and of oxygen are negligible in the time period of few seconds characteristic of the rich event of NSR operation.

3.2. Thermal stability of the stored nitrates and nitrites

The results of TPD experiments of nitrates and nitrites stored onto $Pt–Ba/Al_2O_3$ upon uptake from NO/O_2 at 350 °C and 150 °C are shown in Fig. 2A and C, respectively. These data have already been published [18], but they are here analyzed more into details. In particular, in panels B and D of the same Fig. 2, the instantaneous and integral N/O atomic ratios in the evolved gaseous

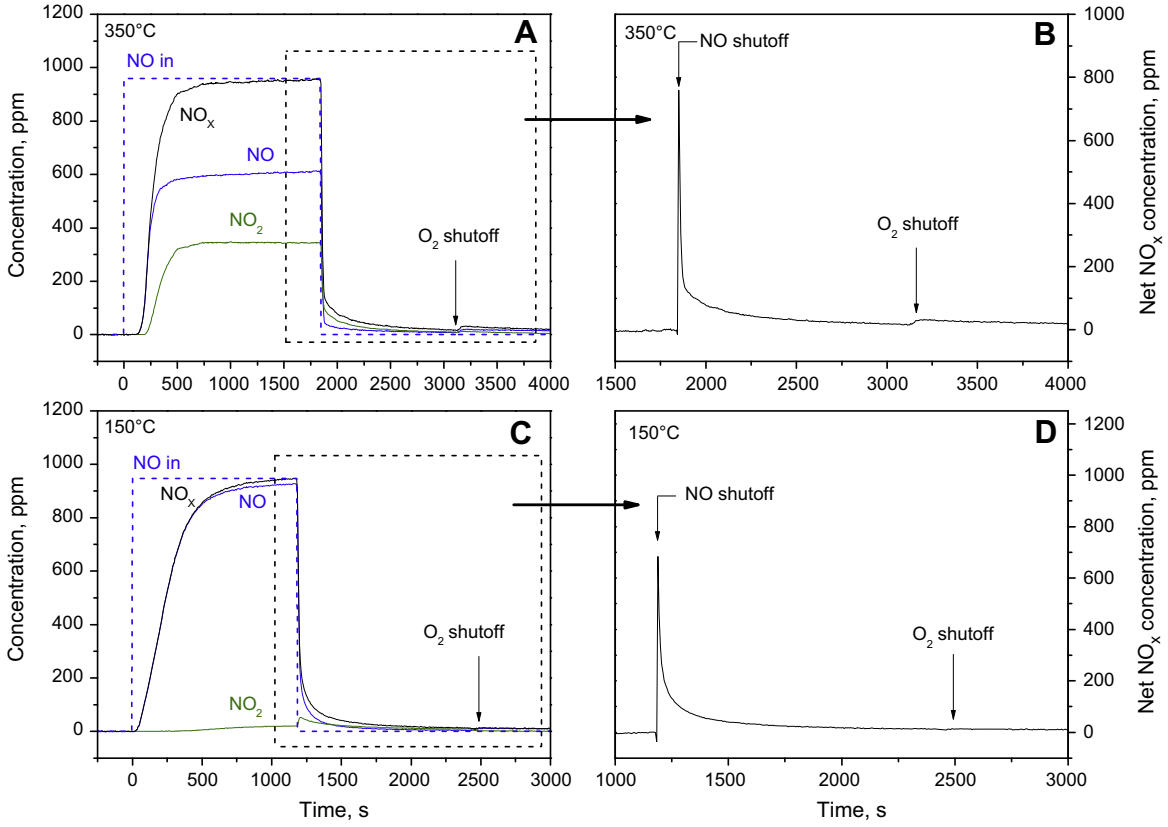

Fig. 1. Effect of NO and O_2 partial pressure on the stability of nitrates and nitrites species stored onto the Pt–Ba/Al_2O_3 catalyst surface. (A) Adsorption phase at 350 °C; (B) NO_x release after NO shutoff at 350 °C; (C) adsorption phase at 150 °C; (D) NO_x release after NO shutoff at 150 °C (storage conditions: 1000 ppm NO + 3% v/v O_2 in He at 350 °C for nitrates or 150 °C for nitrites).

products are reported (panel B and D at 350 °C and 150 °C, respectively).

In the case of nitrates (Fig. 2A), the onset temperature for the decomposition is observed near 320 °C: NO and O_2 represent the major decomposition products, both with maxima centered near 475 °C, along with NO_2 which is detected in lower amount with maximum near 420 °C. Negligible amounts of CO_2 (not shown in figure) are also detected, indicating the presence of residual carbonate species on the catalyst surface after conditioning. During the TPD run and the subsequent hold at 500 °C for about 20 min, nearly all nitrates initially stored desorb from the surface, as pointed out by the subsequent reduction with H_2 accomplished at 350 °C (not shown) where the evolution of very small amount of N_2 has been observed.

The decomposition of nitrates to give NO_2 and NO occurs according to the following reactions:

$$Ba(NO_3)_2 \rightarrow BaO + 2NO_2 + 1/2O_2 \quad (1)$$

$$Ba(NO_3)_2 \rightarrow BaO + 2NO + 3/2O_2 \quad (2)$$

Fig. 2B shows the calculated instantaneous and integral N/O atomic ratio (line a and b, respectively) in the gaseous products during the TPD of nitrates as a function of temperature. It clearly appears that both the instantaneous and integral values keep close to 0.4, that is, the expected ratio for the decomposition of nitrates to NO, NO_2, and O_2 according to the stoichiometry of either reaction (1) or reaction (2).

The results of TPD of nitrites are shown in Fig. 2C. The onset temperature for nitrite decomposition is observed near 125 °C; two NO desorption peaks are observed with maxima centered at 300 °C and 500 °C, this latter corresponding to the end of the heating ramp. The evolution of NO at high temperature is also accompanied by that of O_2, whereas at low temperatures, small amounts of NO_2 are observed. The presence of residual carbonate species on the catalyst surface is confirmed in the case of nitrites as well by the desorption of small amounts of CO_2 (not shown in figure). Also in this case, the desorption of stored NO_x after heating up to 500 °C and subsequent hold at this temperature for about 15 min is almost complete and only minor amounts of N_2 are detected during the subsequent reduction with H_2 at 350 °C (not shown).

In the case of nitrites decomposition, the expected N/O atomic ratio in the evolved products is 0.6, corresponding to the stoichiometry of the reaction:

$$Ba(NO_2)_2 \rightarrow BaO + 2NO + 1/2O_2 \quad (3)$$

However, as apparent from Fig. 2D, the experimental value of the instantaneous N/O atomic ratio changes with temperature being near 1 in the low temperature region and approaching 0.4 in the high temperature region, due to the evolution of NO at low temperatures and of NO and O_2 at high temperatures. The value close to 0.4 at high temperature is in line with the decomposition of nitrates to NO and O_2 provided by reaction (2). On the other hand, the integral value of the N/O atomic ratio keeps close to 1 in the low-temperature region but approaches 0.6 near the end of the run, as expected from the decomposition of nitrites according to the stoichiometry of reaction (3).

To further deepen these aspects, *in situ* FT-IR experiments have been carried out analyzing the adsorption of NO/O_2 at 150 °C followed by the thermal decomposition of the adsorbed species. The IR spectra recorded at various intervals during the uptake from NO/O_2 at 150 °C are shown in Fig. 3A. The storage proceeds with

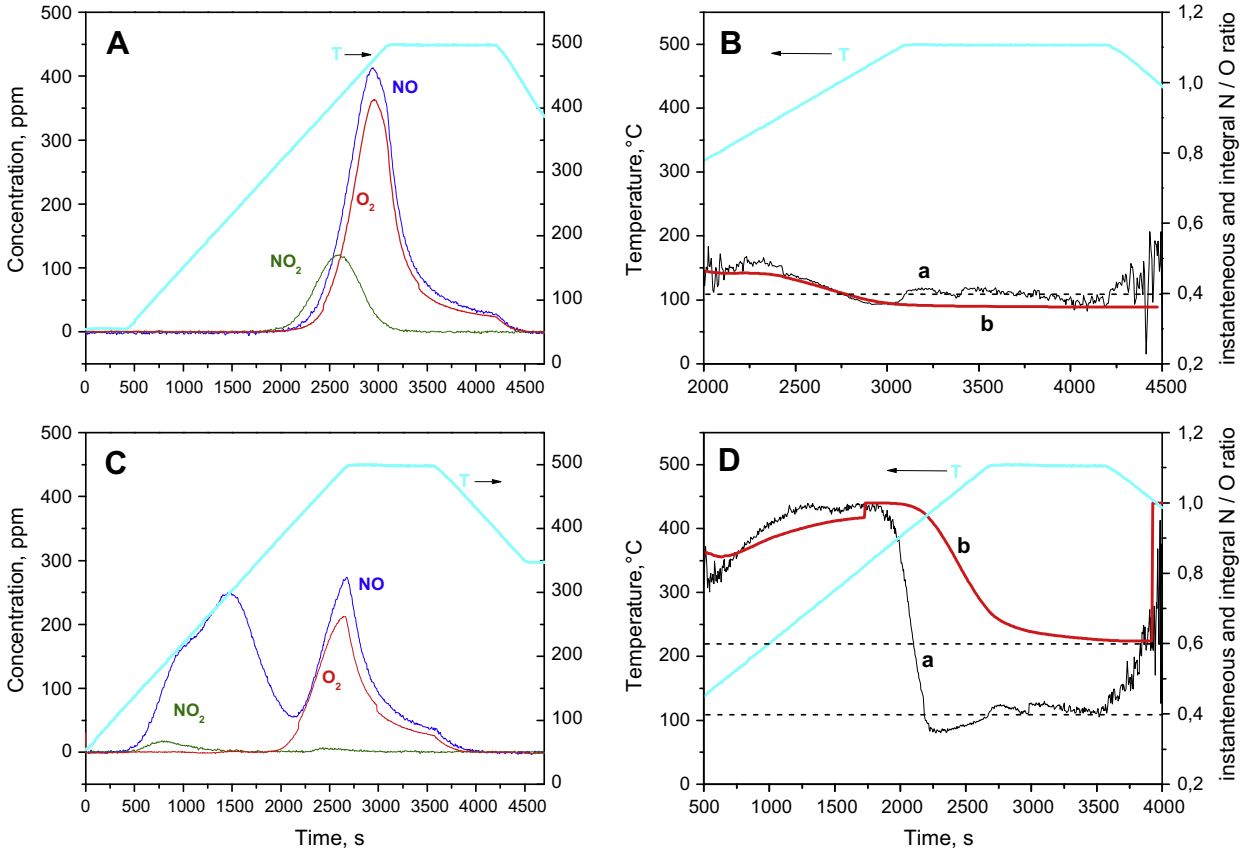

Fig. 2. Thermal decomposition in inert atmosphere (TPD) from 50 to 500 °C (10 °C/min) of nitrates (A) and nitrites (C) species stored onto the Pt–Ba/Al_2O_3 catalyst surface (storage conditions: 1000 ppm NO + 3% v/v O_2 in He at 350 °C for nitrates or 150 °C for nitrites); Instantaneous (line a) and integral (line b) N/O ratio as a function of temperature after storage at 350 °C (B) and after storage at 150 °C (D).

the initial formation of chelating nitrites at the Ba component evidenced by the evolution of the main band at 1217 cm^{-1} ($\nu_{asym.}(NO_2)$ mode), as already pointed out in a previous work [14]. Also the band detected at 1371 cm^{-1} is related to chelating nitrites ($\nu_{sym.}(NO_2)$ mode), although both its shape and position are partially alterate by the presence of residual carbonates at the catalyst surface. The concentration of the surface nitrites increases with the exposure to NO/O_2 until 15 min (Fig. 3A, curve d). A band at 1550 cm^{-1}, possibly associated to bidentate nitrates, is also formed at prolonged exposure time, likely due to the slow nitrites oxidation by oxygen.

FT-IR spectra recorded during the subsequent TPD experiment are shown in Fig. 3B. In this figure, curve a is the spectrum of NO_x species stored at 150 °C, while curves b–h correspond to the spectra recorded at increasing temperatures, up to 500 °C. Of note, the analysis of IR modes is straightforward only at wavenumbers lower than 1300 cm^{-1}, because of the superposition of vibrational modes of carbonates, already present on the sample and/or possibly formed due to the presence of residual amounts of CO_2 in the IR cell. In particular, it is possible to follow the evolution of nitrites through the band at 1217 cm^{-1}. It clearly appears that upon heating the catalyst above 200 °C, chelating nitrites gradually decrease and at 350 °C (Fig. 3B, curve e) they are almost completely removed.

Fig. 3 also shows that, during the removal of nitrites, a new band at 1040 cm^{-1} is detected starting from about 300 °C (see the inset in Fig. 3B, curve d). This band is associated with ionic nitrates ($\nu_{sym.}(NO_3)$ mode) [24,25]. The presence of the other components ($\nu_{asym.}(NO_3)$ modes) of ionic nitrates, which are expected at 1360–1300 cm^{-1} and at 1460–1400 cm^{-1}, is also observed although their evolution cannot be clearly followed due to the superposition with the bands of carbonates. For this reason, the behavior of nitrates can be effectively followed through the mentioned band at 1040 cm^{-1}. In this respect, from the inset of Fig. 3B, it appears that the nitrates start to form at 300 °C, increase with temperature showing a maximum near 350–400 °C (inset in Fig. 3B, curves e, f), then decrease and eventually disappear at 450–500 °C (inset in Fig. 3B, curve g, h).

The FT-IR results, in combination with TPD data of nitrites in Fig. 2 already illustrated, demonstrate that upon heating nitrites are transformed into nitrates with evolution of NO according to the reaction:

$$3Ba(NO_2)_2 \rightarrow Ba(NO_3)_2 + 2BaO + 4NO \uparrow \quad (4)$$

Above 350 °C nitrites are no more present on the catalyst surface and the formed nitrates start to decompose with evolution of NO and O_2, according to the stoichiometry of reaction (2).

In conclusion, the disproportion of nitrites to nitrates and NO (reaction (4)) at low temperatures and the decomposition of nitrates (reaction (2)) above 350 °C explain the decrease with temperature of nitrites with evolution of NO, the formation of nitrates and their decomposition to NO and O_2 above 350 °C.

In line with a previous literature suggestion [15], it can be argued that the decomposition of stored NO_x takes place at the interface between Ba and Pt and that the presence of reduced Pt sites drives this process. Accordingly, it is expected that the formation of Pt–O species (i.e., oxygen adsorbed onto Pt site and/or oxidized Pt site) upon decomposition of the stored NO_x blocks the decomposition process up to high temperature, where oxygen desorbs and metallic Pt sites are restored. Concerning nitrates, the

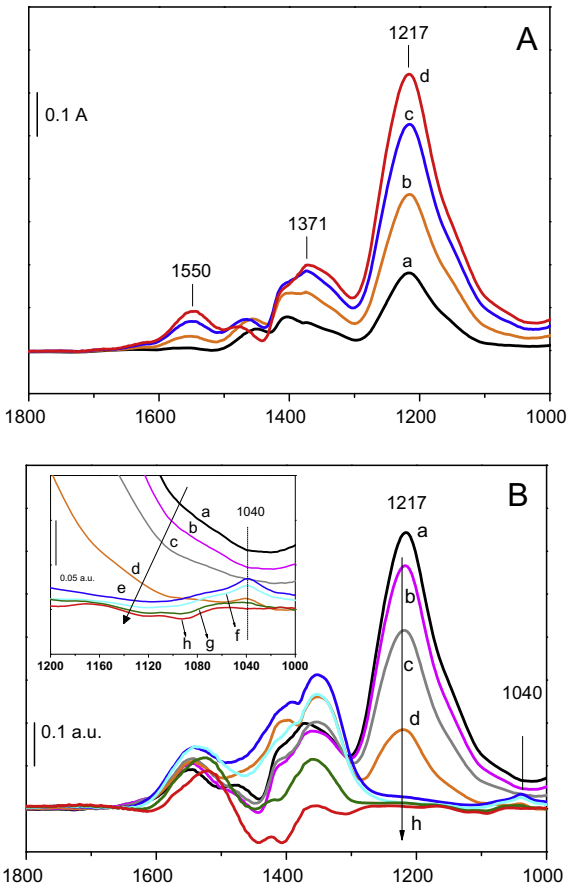

Fig. 3. FT-IR absorbance spectra of NO/O_2 adsorption/desorption over $Pt–Ba/Al_2O_3$, after conditioning at 350 °C. (A) Adsorption of NO/O_2 at 150 °C, spectra taken after (a) 1 min; (b) 5 min; (c) 10 min; (d) 15 min. (B) Spectra recorded during desorption at increasing temperatures under vacuum: (a) 150 °C; (b) 200 °C; (c) 250 °C; (d) 300 °C; (e) 350 °C; (f) 400 °C; (g) 450 °C; (h) 500 °C. The inset in the figure enlarges the 1200–1000 cm^{-1} region.

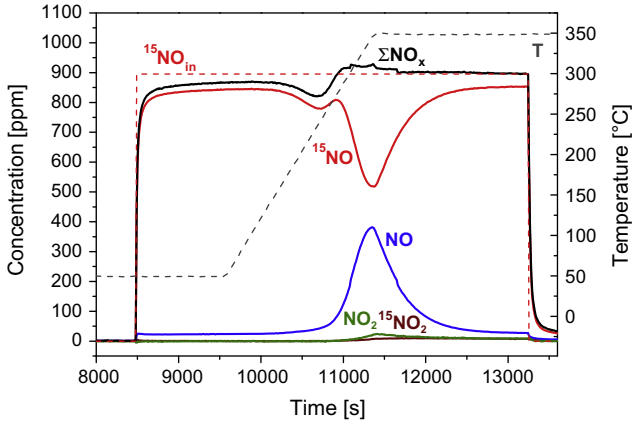

Fig. 4. Isotopic exchange of nitrates run with ^{15}NO (850 ppm) in He from 50 °C to 350 °C, 10 °C/min, after $^{14}NO_x$ adsorption at 350 °C of 1000 ppm NO + O_2 3% v/v in He, over $Pt–Ba/Al_2O_3$ catalyst.

thermal decomposition of these species is seen from 320 °C. In this case, the temperature is high enough so that the Pt–O species, formed upon nitrate decomposition, release oxygen, allowing the nitrates decomposition to proceed. In the case of nitrites, the thermal decomposition occurs from 125 °C and leads to Pt–O species and to the production of gaseous NO. Pt–O species are then involved in the oxidation of nitrites to nitrates, so that no net release of oxygen is observed in the gas phase at low temperature and nitrate species are formed. Accordingly, Pt plays a role in the decomposition of the stored nitrites and in the formation of nitrates as well; the decomposition of stored NO_x is not blocked due to Pt–O formation because these species are consumed to oxidize nitrites into nitrates.

Along similar lines, the tail observed in the NO_x concentration during the NO_x adsorption experiments (Fig. 1) after the NO and O_2 shutoff is associated with the slow decomposition of the stored NO_x at the Pt/Ba interface due to the presence of Pt–O sites.

3.3. Isotopic exchange experiments between ^{15}NO and stored unlabeled nitrates and nitrites

Fig. 4 shows the concentration traces of ^{15}NO, NO, and ΣNO_x (i.e., $^{15}NO + {}^{15}NO_2 + {}^{14}NO + {}^{14}NO_2$) obtained during the ^{15}NO temperature-programmed isotopic exchange (^{15}NO-TPIE) experiment performed with unlabeled nitrates formed upon adsorption of $^{14}NO/O_2$ at 350 °C [14]. Upon admission of ^{15}NO (98% ^{15}N isotopic abundance, see Section 2) at 50 °C, the concentration of ^{15}NO and of impurity ^{14}NO grows up near the inlet value (if one neglects the small adsorption observed at the beginning of the experiment). Hence, no significant isotopic exchange occurs at 50 °C. Upon heating, consumption of ^{15}NO with no desorption of ^{14}NO is initially seen from about 150 °C. Then, between 250 °C and 350 °C consumption of ^{15}NO is observed, accompanied by a correspondent release of ^{14}NO. Small amounts of unlabeled and labeled NO_2 are also detected starting from 260 °C; oxygen is not observed among the products at any temperature.

The first consumption of ^{15}NO from 150 °C can be ascribed to weak adsorption of $^{15}NO_x$ on Ba sites, possibly due to superficial oxygen present after the uptake at 350 °C with $^{14}NO/O_2$ followed by the He purge [26]. At variance, the second ^{15}NO consumption peak in the 250–350 °C temperature range is accompanied by a correspondent evolution of ^{14}NO, and it is almost not associated with changes in the concentration of the total gaseous NO_x species (ΣNO_x), nor with a release of O_2. Accordingly, if one neglects the evolution of small amounts of NO_2, the exchange between labeled gas phase ^{15}NO and unlabeled stored nitrates is described by the following reaction:

$$Ba(^{14}NO_3)_2 + 2{}^{15}NO \rightarrow Ba(^{15}NO_3)_2 + 2{}^{14}NO\uparrow \quad (5)$$

The exchange between NO and stored nitrates is observed from a temperature well below that of thermal decomposition of stored nitrates measured by TPD in He illustrated in the previous paragraph in Section 3.2 (i.e., from about 250 °C vs. 320 °C). The exchange reaction proceeds up to 350 °C and during the subsequent hold at this temperature for 30 min under flow of ^{15}NO in He. After the ^{15}NO shutoff, a tail in ^{15}NO concentration is observed, revealing that labeled weakly adsorbed species are desorbing from the catalyst surface. Then, the catalyst has been regenerated with H_2 at 350 °C (not shown) and only species containing labeled nitrogen atoms, that is, $^{15}N_2$ and small quantities of $^{15}NH_3$, have been observed among the products. Trace amounts of $^{15}N^{14}N$ have also been formed, ascribed to the presence of ^{14}NO impurity in the ^{15}NO cylinder (see Section 2). This proves that only labeled $^{15}NO_x$ species are stored onto the catalyst at the end of the ^{15}NO-TPIE experiment, so that the exchange was complete.

^{15}NO-TPIE experiment has also been performed after adsorption of $^{14}NO/O_2$ at 150 °C, leading to the formation of unlabeled nitrites [14], and results are shown in Fig. 5. Consumption of ^{15}NO is observed immediately upon admission at 50 °C. During the first 100 s, the ^{15}NO consumption keeps constant and a correspondent evolution of unlabeled ^{14}NO is observed. Subsequently, the

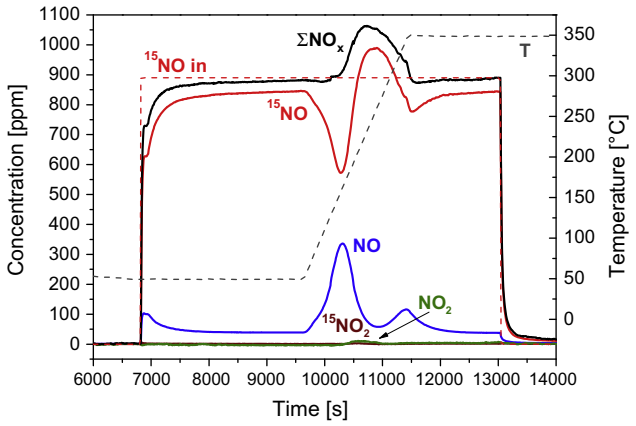

Fig. 5. Isotopic exchange of nitrites run with ^{15}NO (850 ppm) in He from 50 °C to 350 °C, 10 °C/min, after $^{14}NO_x$ adsorption at 150 °C of 1000 ppm NO + O_2 3% v/v in He, over Pt–Ba/Al_2O_3 catalyst.

concentrations of ^{15}NO increase and that of ^{14}NO decrease to the inlet concentration values (^{15}N isotopic abundance in the ^{15}NO/He cylinder 98%, see Section 2), while the temperature is maintained at 50 °C.

By considering that no changes in the inlet concentration of the total gaseous NO_x species (ΣNO_x) are observed at this temperature (if one neglects the small adsorption observed at the beginning of the experiment), the exchange between labeled ^{15}NO and unlabeled stored nitrites is described by the following reaction:

$$Ba(^{14}NO_2)_2 + 2\,^{15}NO \rightarrow Ba(^{15}NO_2)_2 + 2\,^{14}NO\uparrow \quad (6)$$

This reaction is already effective at 50 °C, which is well below the onset temperature of the thermal decomposition of stored nitrites measured by TPD in He and illustrated in the previous paragraph in Section 3.2 (i.e., 50 °C vs. 125 °C). It has been calculated that at 50 °C, before the start of the heating ramp, roughly 22% of the initially stored NO_x have been exchanged. Upon increasing the temperature, the reaction further proceeds and a maximum in the consumption of labeled ^{15}NO, together with the correspondent release of unlabeled ^{14}NO, is observed with maximum at 150 °C.

Then, above this temperature, the ^{14}NO concentration decreases and an increase is observed in the ^{15}NO concentration trace. Notably, the ^{15}NO concentration at the exit of the reactor exceeds the inlet ^{15}NO concentration above 200 °C with a maximum near 250 °C. In addition, the overall NO_x concentration trace (ΣNO_x) exceeds the inlet concentration of NO above 150 °C with maximum at 250 °C. These results can be explained as follows: the stored unlabeled nitrites start to be exchanged already at 50 °C and during subsequent heating up to 130–150 °C as well, leading to ^{15}NO consumption and ^{14}NO evolution. Above 130–150 °C, the partially exchanged stored nitrites decompose according to reaction (4), so that the overall NO_x concentration (ΣNO_x) exceeds the inlet NO concentration value while nitrates are formed. The onset temperature of nitrites decomposition in Fig. 5 compares well with that observed during TPD of nitrites in Fig. 2C, being slightly higher (130–150 °C vs. near 125 °C) because of the more oxidizing environment. Above 250 °C and during the initial part of the hold at 350 °C under flow of ^{15}NO in He the so-formed nitrates are exchanged, in line with the results of ^{15}NO-TPIE experiment of nitrates previously discussed (Fig. 4). Accordingly, at the end of the run only exchanged nitrates are expected to be present on the catalyst surface, in line with FT-IR data previously shown (Fig. 3).

After the ^{15}NO shutoff, a tail in ^{15}NO concentration reveals that labeled weakly adsorbed species are desorbing [19,26]. During the subsequent catalyst regeneration with H_2 at 350 °C (not shown), only the formation of labeled-containing products has been observed, like in the ^{15}NO-TPIE experiment of nitrates previously discussed. Negligible amounts of $^{15}N^{14}N$ have also been detected due to the isotopic abundance of ^{15}NO in the cylinder (98%; see Section 2).

In order to clarify the role of the noble metal in this process, a ^{15}NO-TPIE experiment has been performed over a Pt-free Ba/Al_2O_3 sample. Nitrates have been stored at 350 °C starting from unlabeled $^{14}NO_2$; then after cooling to 50 °C, labeled ^{15}NO has been admitted to the reactor and the temperature was increased up to 350 °C. The results, reported in Fig. 6 show that the isotopic exchange reaction occurs only to a negligible extent; in fact, only small amounts of ^{14}NO (with a peak maximum of near 25 ppm) are desorbed at 350 °C. This demonstrates that Pt is involved in the exchange reaction. In another experiment, a ^{15}NO-TPIE run has been performed over the Pt–Ba/Al_2O_3 catalyst with stored nitrites after the Pt sites have been poisoned with CO admitted at 50 °C. The results of the ^{15}NO-TPIE experiment carried out after Pt poisoning by CO at 50 °C are shown in Fig. 7 as solid lines, where they are compared with the results of the ^{15}NO-TPIE experiment of nitrites accomplished over the un-poisoned catalyst (dashed lines).

After poisoning of Pt by CO both the consumption of ^{15}NO and the correspondent release of ^{14}NO at 50 °C are significantly decreased. In fact, the amount of NO_x exchanged in the same time period (i.e., the initial 1330 s after the ^{15}NO inlet) decreases from 11% to 4%. Accordingly, when Pt sites are poisoned by CO with formation of Pt carbonyls, the isotopic exchange at 50 °C is inhibited. This confirms the role of Pt in the reaction. Only above 70 °C, likely corresponding to the desorption/oxidation of CO, the consumption of ^{15}NO and the correspondent production of ^{14}NO are detected, indicating the occurrence of the exchange reaction. As a matter of fact, about 10 ppm of CO_2 have been detected among the reaction products. From this temperature onwards the amounts of ^{15}NO exchanged well compare with those calculated over the un-poisoned catalyst, indicating that the isotopic exchange reaction is delayed because the Pt sites are blocked by CO at low temperatures.

The importance of Pt during the ^{15}NO isotopic exchange has also been pointed out by Cant and coworkers [15] when studying the exchange between ^{15}NO and stored NO_x over Pt–BaO/Al_2O_3 and over Pt/SiO_2 physically mixed with BaO/Al_2O_3 in the presence of 2% O_2. These authors found that the exchange was much more rapid over Pt–BaO/Al_2O_3 than over the combined system, that is, is faster when Pt and BaO are located over the same support than in systems where Pt is placed separately from BaO (or it is absent).

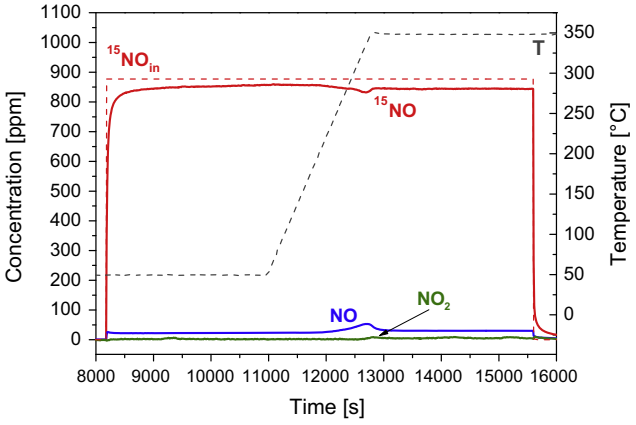

Fig. 6. Isotopic exchange run with ^{15}NO (850 ppm) in He from 50 °C to 350 °C, 10 °C/min, after NO_2 adsorption at 350 °C of 1000 ppm NO_2 + O_2 3% v/v in He, over Ba/Al_2O_3 catalyst.

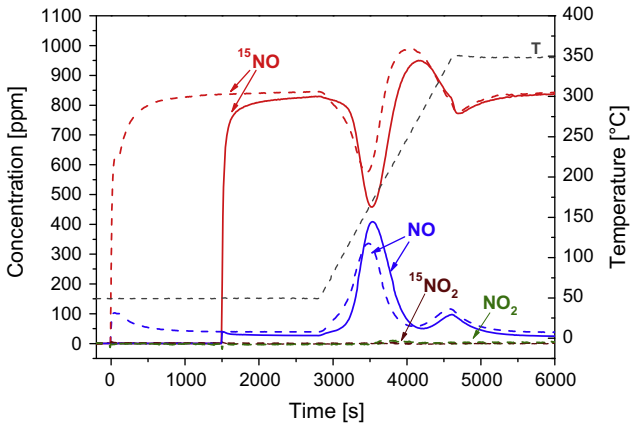

Fig. 7. Isotopic exchange of stored unlabeled nitrites run with ^{15}NO (850 ppm) in He from 50 °C to 350 °C, 10 °C/min (dashed lines), and after CO dosing with 2000 ppm of CO at 40 °C (solid lines), over Pt–Ba/Al_2O_3 catalyst.

Similar conclusions have been reached by Kumar et al. [16] who suggested that the isotopic ^{15}NO exchange takes place at the Pt/BaO interface.

Hence, the ^{15}NO isotopic exchange experiments here reported, which imply the release of stored NO_x, have shown that: (i) the exchange reaction is observed from a temperature well below that of thermal decomposition of stored NO_x, that is, from about 50 °C vs. 125 °C for nitrites and from 250 °C vs. 320 °C for nitrates; (ii) Pt is necessary for the exchange because this is observed over Pt–Ba/Al_2O_3 but not over Ba/Al_2O_3 and is inhibited by CO at low temperature due to poisoning of Pt with formation of Pt carbonyls; (iii) all stored NO_x have been exchanged at 350 °C. This implies the reverse spillover of the NO_x stored onto the Ba component far from Pt, if any, to the Pt metal sites. Nevertheless, the reverse spillover is expected to be of minor importance over catalysts with high Pt dispersion (above 50%), such as that used in this study.

The mechanism we suggest for NO isotopic exchange is sketched in Fig. 8. Upon interaction of unlabeled NO_x species stored at a Ba site with a neighboring metallic Pt site, unlabeled NO is released in the gas phase and a free BaO site is formed, while adsorbed oxygen is left at Pt site, leading to oxygen adsorbed on Pt and/or to oxidized Pt site (Pt–O). In the absence of a reductant, which scavenges the adsorbed oxygen atoms from the Pt sites, the process cannot proceed further. Indeed, this is what is seen during the TPD of nitrates where decomposition is observed only at high temperatures, once O-adatoms are released as O_2 in the gas phase. During TPD of nitrites, where decomposition occurs at lower temperatures than for nitrates, oxygen is scavenged by other nitrites with formation of nitrates.

When ^{15}NO is present in the gas phase, adsorbed oxygen atoms are scavenged from Pt sites by ^{15}NO, leading to the formation of labeled nitrites/nitrates adsorbed species (see bottom of Fig. 8). Hence, the exchange occurs between gas-phase ^{15}NO and stored $^{14}NO_x$ and it can be monitored by using labeled molecules as in the case of ^{15}NO-TPIE experiments.

A tentative reaction scheme of NO isotopic exchange is given below, where the participation of Pt and Pt–O species is envisaged:

$$Ba(^{14}NO_3)_2 + 2Pt \rightarrow Ba(^{14}NO_2)_2 + 2Pt{-}O \quad (7)$$

$$Ba(^{14}NO_2)_2 + Pt \rightarrow BaO + 2\,^{14}NO\uparrow + Pt{-}O \quad (8)$$

$$2\,^{15}NO + Pt{-}O + BaO \rightarrow Ba(^{15}NO_2)_2 + Pt \quad (9)$$

$$Ba(^{15}NO_2)_2 + 2\,Pt{-}O \rightarrow Ba(^{15}NO_3)_2 + 2\,Pt \quad (10)$$

Nitrates and nitrites are reduced at metallic Pt sites leading to NO evolution and formation of Pt–O species (reactions (7) + (8) and (8), respectively). The Pt–O species oxidize labeled NO present in the gas phase to give adsorbed labeled nitrite and nitrate species and restoring the metallic Pt sites (reactions (9) and (9) + (10), respectively). The intermediacy of nitrites in the reduction of nitrates and in the oxidation of NO is assumed in view of their higher reactivity in the isotopic exchange between NO and stored NO_x. It is worth noting that the NO isotopic exchange is a redox process where metallic Pt centers activate stored nitrites and nitrates that are destabilized and eventually released in the gas phase as NO. The released NO cannot be further reduced due to the lack of reducing agents, and this makes ^{15}NO isotopic exchange experiments suitable for decoupling the NO_x release driven by metallic Pt sites from its further reduction.

It is worth of note that in the previous scheme (reactions (7)–(10)) Pt–Ba couples are involved, pointing out the occurrence of interfacial reactions. Since all the stored NO_x have been exchanged, this implies the reverse spillover of nitrites and nitrates stored onto the BaO component far from Pt, if any, to the Pt metal sites. In fact, as discussed above, the catalyst has a rather high dispersion, implying a large interfacial contact between the Pt and the Ba component.

3.4. The role of the reducing agent in the NO_x release

As discussed before, the NO_x release is a chemical reaction occurring at the Pt/Ba interface and driven by metallic Pt centers. Therefore, it is expected that the release of stored NO_x is favored in the presence of a reductant, due to the formation of reactive metallic Pt centers. The reactivity of stored nitrates with different reducing agents (H_2, NH_3, CO, and n-heptane) has been previously studied by TPSR experiments [18,23,27]. Notably, at variance to the case of isotopic exchange between ^{15}NO and stored $^{14}NO_x$, during

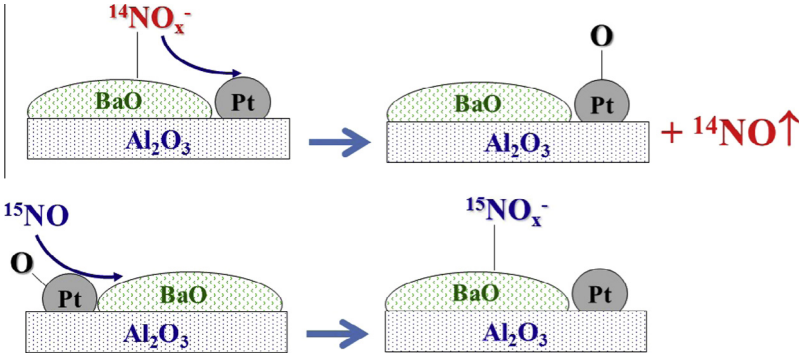

Fig. 8. Sketch of the mechanism of ^{15}NO isotopic exchange.

TPSR experiments (i.e., when a reducing agent for NO is present in the feed) the release of stored NO_x cannot be decoupled from their further reduction. The results of these TPSR experiments are here revisited in order to clarify the role of the reductant in the reduction of stored NO_x, that is, in the release of NO_x and in their further reduction. In Fig. 9, the concentrations of the reducing agent, of NO and of the other N-containing products quoted as ΣN (which include N_2, NH_3 and traces of N_2O), are shown as a function of temperature. The onset temperature of the ^{15}NO isotopic exchange of nitrates ($T_{exchange}$) is also shown in the figure as dashed line.

When hydrogen is employed as reducing agent (Fig. 9A), its consumption is observed starting from slightly below 150 °C. Evolution of the reaction products is seen at slightly higher temperatures near 160 °C, which suggests that hydrogen is initially involved in the adsorption at/reduction of the Pt sites before nitrates are being reduced; N_2 and NH_3 but not NO neither N_2O are observed among the products. Notably, the onset temperature of the reduction of nitrates is much lower than that of the isotopic exchange between ^{15}NO and unlabeled nitrates (i.e., near 150–160 °C vs. 250 °C, see Fig. 9).

When NH_3, CO, or n-heptane are used as reducing agents (Fig. 9B, C and D, respectively), similar results are obtained, although different onset temperatures are observed for the reduction of stored nitrates. In the case of NH_3 (Fig. 9B), the onset temperature of its consumption cannot be accurately determined because is superimposed to NH_3 desorption upon heating after NH_3 adsorption at 50 °C while evolution of the reduction products is seen near 150 °C.

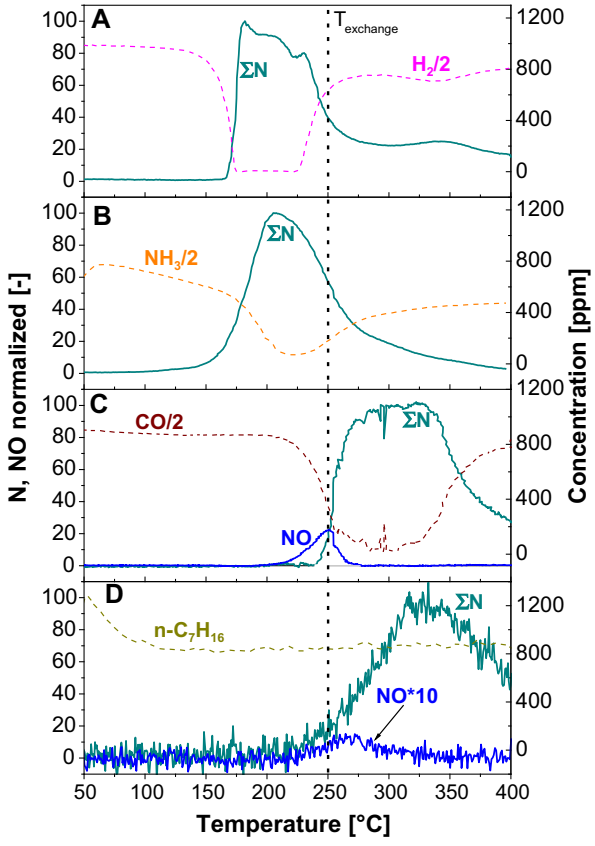

Fig. 9. TPSR experiments over Pt–Ba/Al_2O_3 from 50 °C to 400 °C, 10 °C/min, feeding: (A) 2000 ppm of H_2; (B) 1000 ppm of NH_3; (C) 1000 ppm of CO; (D) 910 ppm of n-heptane, after $^{14}NO_x$ adsorption at 350 °C of 1000 ppm NO + O_2 3% v/v in He. ΣN quotes N-containing products (which include N_2, NH_3 and traces of N_2O); $T_{exchange}$ represents the onset temperature of the ^{15}NO isotopic exchange of nitrates.

In the case of CO (Fig. 9C) and of n-heptane (Fig. 9D), the onset temperature of products evolution is shifted towards higher temperature, that is, near 200 °C and 230 °C, respectively, but it is still lower than that of NO isotopic exchange, near 250 °C. Notably, the onset temperature for CO consumption is slightly lower than that of the product evolution, like in the case of H_2. On the other hand, no consumption is seen in the case of n-heptane due to its high concentration. The higher onset temperatures observed in the case of CO-TPSR and n-heptane-TPSR with respect to H_2-TPSR and NH_3-TPSR is due to the lower reactivity of CO and n-heptane in the O_{ads} removal from Pt sites, in line with previous literature reports [28,29].

The following order is observed for the onset temperature of the release and reduction of stored NO_x: $T(H_2) \approx T(NH_3) < T(CO) < T(n\text{-}C_7H_{16}) < T(NO)$. This order compares fairly well with the efficiency of the reductants in scavenging the O-adatoms from Pt–O and then in the activation of stored NO_x by Pt reduced centers, that seems to represent the rate determining step of the reduction of stored NO_x.

Considering the nature of the reduction products, it is worth to note that in the case of CO and of n-heptane NO is detected in very small amounts among the products at near the onset of the reduction process. In the case of n-heptane in addition to NO traces of N_2O are detected as well. At variance, NO and N_2O are not observed among the products in the case of H_2 and NH_3. Indeed, in the presence of efficient reductants like H_2 and NH_3, it is likely that NO formed upon the activation of stored nitrates does not desorb from Pt, but is readily decomposed to N- and O-adatoms over the metal Pt sites. Once formed, O-adatoms are scavenged by H-adatoms formed upon decomposition of H_2 and of NH_3 with formation of H_2O whereas N-adatoms combine to form N_2 or are hydrogenated to give NH_3 (in the case of H_2), which are indeed observed among the reaction products [18]. However, it is not possible to exclude that NO might be released in the gas phase and subsequently re-adsorbed and decomposed at metal Pt sites to give N_2 and NH_3. As a matter of fact, the onset temperature for the reaction between gaseous NO and the reducing agent is always lower than that of the reduction of the stored nitrates, namely near 40 °C vs. 150–160 °C for H_2 [30], near 100 °C vs. near 150 °C for NH_3 [27], near 160 °C vs. 200 °C for CO [31], and near 180 °C vs. 230 °C for n-heptane [32].

When the reactivity of the reductant is lower, like in the case of CO and of n-heptane, Pt–O is less efficiently reduced to metal Pt and NO is observed among the products. This explains (i) the higher temperature of onset for the reduction of the stored nitrates; (ii) the release in the gas phase of NO formed upon the reduction of the stored NO_x, being NO not readily decomposed into N- and O-adatoms over partially O-covered Pt site. The detection of traces of N_2O in the case of n-heptane is also in line with the poor reactivity of this reductant, being N_2O formation favored in the presence of oxidized Pt sites [22,33]. Upon increasing the temperature, the evolution of NO (and of N_2O) is no more observed, because CO and n-heptane efficiently scavenge O-adatoms from Pt, and this favors NO decomposition to N- and O-adatoms and subsequent coupling of N-adatoms to give N_2.

In view of the suggested picture, the regeneration process is built on a complex sequence of steps: after reduction of the noble metal sites, the stored NO_x species at the Pt/Ba interface are released as NO_x or NO_x-related intermediates (in the gas phase or adsorbed over Pt), which are converted to different products according to the oxidation state of Pt. In this regard, it is likely that both the reduction of Pt sites and the release of NO_x from the stored NO_x affects the rate of the reduction process. Indeed, by using efficient reductants ($H_2 > NH_3 > CO > n\text{-}C_7H_{16}$), the onset for the reduction of stored NO_x is shifted to lower temperatures. Besides, when an efficient reductant is used at high concentrations, the NO_x supply at the reduced Pt sites becomes the rate determining step: released NO_x are readily reduced at Pt sites into products

like N_2 or NH_3 (in the case of H_2 as reductant). This is expected to be the case also for NO_x species stored on Ba sites far away from Pt, whose reactivity involves the reverse spillover from Ba to Pt sites. At variance, when the reactivity of the reductant is poor or the local reductant concentration is small, the NO_x released are not efficiently reduced and this results in the evolution of NO_x (and N_2O as well) in the gas phase, as in fact observed in the case of CO and n-C_7H_{16} TPSR experiments.

As a final remark, for NO_x species stored on Ba sites far away from Pt, the potential spillover of H-, CO-, and C_xH_y- fragments towards the adsorbed NO_x species and the subsequent reaction with the stored NO_x has been also suggested [11,12,34]. However, this pathway is apparently a less-efficient route for the removal of the stored NO_x over our catalyst. As a matter of fact, TPSR experiments carried out with Pt/Al_2O_3–Ba/Al_2O_3 mechanical mixture pointed out that NO_x stored onto the Ba/Al_2O_3 sample could not be reduced in spite of the fact that H_2 activated over Pt/Al_2O_3 could migrate to the Ba/Al_2O_3 particles [19].

4. Conclusions

In this work, the release and reduction of stored NO_x over Pt–Ba/Al_2O_3 has been investigated. The following main conclusions have been obtained:

(i) The release of stored NO_x driven by adsorption–desorption equilibrium and caused by the decrease in the partial pressure of NO and/or of O_2 upon the lean/rich switch is negligible under typical NSR operation.

(ii) The release of stored NO_x has been decoupled from their further reduction by performing isotopic exchange experiment between labeled ^{15}NO and stored unlabeled nitrates and nitrites, so that the process of NO_x release has been characterized unambiguously. The exchange reaction implies the release of stored NO_x, is catalyzed by Pt, is observed from temperatures well below those of thermal desorption of stored NO_x measured during TPD in He, and is complete at 350 °C. The exchange between ^{15}NO and stored unlabeled nitrates and nitrites is a redox process: it is suggested that the reduced Pt sites activate stored NO_x species that are destabilized and eventually released in the gas phase, as NO.

(iii) Metal Pt centers drive the NO_x release from the stored NO_x, and in fact, is favoured by the presence of a reductant. The following order is observed for the onset temperature of the release and reduction of the stored NO_x: $T(H_2) \approx T(NH_3) < T(CO) < T(n\text{-}C_7H_{16}) < T(NO)$. This order well compares with the efficiency of the reductant in the scavenging of O-adatoms from Pt–O and then in the activation of stored NO_x by Pt reduced centers that represent the rate determining steps of the release and reduction of stored NO_x. Therefore, under nearly isothermal conditions, the NO_x release is a chemical reaction catalyzed by Pt occurring at the Pt/Ba interface.

(iv) In the presence of strong reductant (e.g., H_2 or NH_3), NO_x released from the stored NO_x are reduced before they are desorbed. However, it cannot be excluded that NO might be released in the gas phase and subsequently re-adsorbed and decomposed at metal Pt sites to give eventually N_2 and other by-products. At variance, in the presence of weak reductant (e.g., CO or n-heptane) NO_x are released in the gas phase upon activation of the stored NO_x, but not readily decomposed into N- and O-adatoms over partially O-covered Pt site leading to NO evolution. The detection of small amounts of N_2O is also in line with the poor reducing power of the reductant, being N_2O formation favored in the presence of oxidized Pt sites.

Acknowledgments

The authors are grateful to Dr. Sara Morandi, University of Torino, for interpretation of FT-IR spectra and stimulating discussion.

References

[1] <http://delphi.com/manufacturers/auto/powertrain/emissions_standards/>, 2014.
[2] T. Johnson, Platinum Metals Rev. 52 (1) (2008) 23.
[3] M.V. Twigg, Platinum Metals Rev. 57 (3) (2013) 192.
[4] W.S. Epling, I.E. Campbell, A. Yezerets, N.W. Currier, J.E. Park, Catal. Rev. Sci. Eng. 46 (2004) 163.
[5] K.S. Kabin, R.L. Muncrief, M.P. Harold, Catal. Today 96 (2004) 79.
[6] R.L. Muncrief, K.S. Kabin, M.P. Harold, AIChE J. 50 (2004) 2526.
[7] A. Amberntsson, H. Persson, P. Engström, B. Kasemo, Appl. Catal. B: Environ. 31 (2001) 27.
[8] Z. Liu, J.A. Anderson, J. Catal. 224 (2004) 18.
[9] N.W. Cant, M.J. Patterson, Catal. Lett. 85 (2003) 153.
[10] S. Poulston, R. Rajaram, Catal. Today 81 (2003) 603.
[11] B.M. Shakya, M.P. Harold, V. Balakotaiah, Catal. Today 184 (2012) 27.
[12] R.D. Clayton, M.P. Harold, V. Balakotaiah, C.Z. Wan, Appl. Catal. B: Environ. 90 (2009) 662.
[13] B. Westerberg, E. Fridell, J. Mol. Catal. A: Chem. 165 (2001) 249.
[14] L. Lietti, M. Daturi, V. Blasin-Aubé, G. Ghiotti, F. Prinetto, P. Forzatti, Chem. Cat. Chem. 4 (2012) 55.
[15] N.W. Cant, I.O.Y. Liu, M.J. Patterson, J. Catal. 243 (2006) 309.
[16] A. Kumar, M.P. Harold, V. Balakotaiah, J. Catal. 270 (2010) 214.
[17] N. Miyoshi, T. Tanizawa, K. Kasahara, S. Tateishi, European Patent Application 0 669 157 A1, 1995.
[18] A. Infantes-Molina, L. Righini, L. Castoldi, C.V. Loricera, J.L.G. Fierro, A. Sin, L. Lietti, Catal. Today 197 (2012) 178.
[19] I. Nova, L. Castoldi, L. Lietti, E. Tronconi, P. Forzatti, SAE Technical Paper 2006-1-1368.
[20] L. Lietti, P. Forzatti, I. Nova, E. Tronconi, J. Catal. 204 (2001) 175.
[21] S. Morandi, F. Prinetto, G. Ghiotti, L. Castoldi, L. Lietti, P. Forzatti, M. Daturi, V. Blasin-Aubé, Catal. Today 231 (2014) 116.
[22] L. Lietti, N. Artioli, L. Righini, L. Castoldi, P. Forzatti, Ind. Eng. Chem. Res. 51 (2012) 7597.
[23] I. Nova, L. Lietti, L. Castoldi, E. Tronconi, P. Forzatti, J. Catal. 239 (2006) 244.
[24] F. Prinetto, G. Ghiotti, I. Nova, L. Lietti, E. Tronconi, P. Forzatti, J. Phys. Chem. B 105 (2001) 12732.
[25] S. Morandi, F. Prinetto, L. Castoldi, L. Lietti, P. Forzatti, G. Ghiotti, Phys. Chem. Chem. Phys. 15 (2013) 13409.
[26] I. Nova, L. Castoldi, L. Lietti, E. Tronconi, P. Forzatti, F. Prinetto, G. Ghiotti, J. Catal. 222 (2004) 377.
[27] L. Castoldi, L. Lietti, L. Righini, P. Forzatti, S. Morandi, G. Ghiotti, Top. Catal. 56 (2013) 193.
[28] H. Abdulamid, E. Fridell, M. Skoglundh, Top. Catal. 30 (31) (2004) 161.
[29] C.D. Di Giulio, V.G. Komvokis, M.D. Amiridis, Catal. Today 184 (2012) 8.
[30] L. Castoldi, I. Nova, L. Lietti, E. Tronconi, P. Forzatti, Top. Catal. 42–43 (2007) 189.
[31] Unpublished results.
[32] L. Righini, L. Kubiak, S. Morandi, L. Castoldi, L. Lietti, P. Forzatti, ACS Catal. 4 (2014) 3261.
[33] V.A. Kondraratenko, M. Baerns, Appl. Catal. B: Environ. 70 (2007) 111.
[34] J.-Y. Luo, W.S. Epling, Appl. Catal. B: Environ. 97 (2010) 236.